Iraqi J. Laser, Part A, Vol.17, pp.1-8 (2018)

IRAQI JOURNAL OF LASER

# Enhancement the Sensitivity of Humidity Sensor Based on an Agarose Coating Transmission-Type Photonic Crystal Fiber Interferometer

**Hassan F. Hassan** and **Hanan J. Taher**

*Institute of Laser for Postgraduate Studies, University of Baghdad, Baghdad, Iraq*
*E-mail:hsnfaleh@gmail.com*

(Received 10 September 2017; accepted 2 November 2017)

**Abstract:** Photonic Crystal Fiber Interferometers (PCFIs) are widely used for sensing applications. This work presents the fabrication and the characterization of a relative humidity sensor based on a polymer-coated photonic crystal fiber that operates in a Mach- Zehnder Interferometer (MZI) transmission mode. The fabrication of the sensor involved splicing a short (1 cm) length of Photonic Crystal Fiber (PCF) between two single-mode fibers (SMF). It was then coated with a layer of agarose solution. Experimental results showed that a high humidity sensitivity of 29.37 pm/%RH was achieved within a measurement range of 27–95%RH. The sensor also showed good repeatability, small size, measurement accuracy and wide humidity range. The RH sensitivity of the sensor has a significant dependence on the thickness of the coating and the sensor with the highest sensitivity showed a linear response for RH change in the range of 27-95% RH and a fast response time of 0.8 sec for an RH change from 50% to 90%.

***Keywords:*** *Agarose, Humidity measurement, Mach-zender interferometer, Transition mode, Photonic crystal fiber.*

## Introduction

Humidity is a physical quantity that has significant importance in a number of areas ranging from life sciences [1,2] to building automation [3]. Hence humidity control, sensing and monitoring are important in a number of areas. Fast humidity sensors are required for the diagnosis of pulmonary diseases [4] and for mapping the human respiratory system [5] by monitoring the water vapor content of exhaled breath. For meteorological applications, humidity measurements play an ever-increasing role in various industries such as semiconductor, bio-medical, agricultural, food processing, automotive and meteorological industries. These measurements are important to allow improvements in the quality of products and reduction of costs. For over a decade, fiber optic humidity sensors have gained a lot of research interest due to their unique advantages over conventional electronic ones. For example, they are miniature in size and immune to electromagnetic interference. A variety of fiber humidity sensors have been demonstrated based on different fiber types and configurations, including tapered fibers [6], bent fibers [7], polarization maintaining fibers [8, 9], fiber gratings [10–11] and no-core fibers [12]. Most fiber optic humidity sensors work on the basis of a hygroscopic polymer material coated over the optical fiber to modulate the light propagating through the fiber [13–14]. Recently photonic crystal fiber (PCF) interferometers based on microhole collapse have taken an increased importance in sensing applications [15–16] due to their fabrication simplicity which involves only cleaving and splicing operations. The different configurations reported so far are the PCF with two collapsed regions separated by a few centimeters [17], a stub of PCF with the cleaved end fusion spliced to the distal end of a standard single mode fiber [18–19] and a short section of PCF longitudinally sandwiched between single mode fibers [17–20]. The advantage of the last two configurations is that the modal properties of the PCF are exploited but conventional optical fibers are used to

connect the interrogation system, thus leading to more cost-effective interferometers. In photonic crystal fiber interferometer(PCFI) configuration in which the two ends of a PCF are fusion spliced to lead-in and lead-out, single mode fibers have already been demonstrated for strain [17,20] and refractive index(RI) [21] sensing. A humidity sensor based on this type of PCFI configuration using an Agarose coating has been recently demonstrated for the first time [22]. The RH sensitivity of the sensor was 8 pm/%RH in the range 30-80%RH. The aim of this work is to improve the sensitivity of this type of RH sensor by coating with Agarose solution.

**Fabrication and Experimentation**

The PCF (LMA-10, NKT Photonics) designed for an endless single–mode operation was used. It had six layers of air holes arranged in a hexagonal pattern around a solid silica core. The fiber had core diameter of 10.2μm, voids with diameter 2.5 μm, pitch of 8.07 μm and the outer diameter of 125 μm. These dimensions of the PCF alignment and splicing with SMF with splicing machine and due to mode-field diameter (MFD) mismatch compared to other PCFs. The loss was minimized during the splicing process and due to surface tension. The voids of the PCF collapsed within a microscopic region (~247μm ) near the splice point which can be controlled by the arc time, arc power and duration[26], as shown in Figure 1.

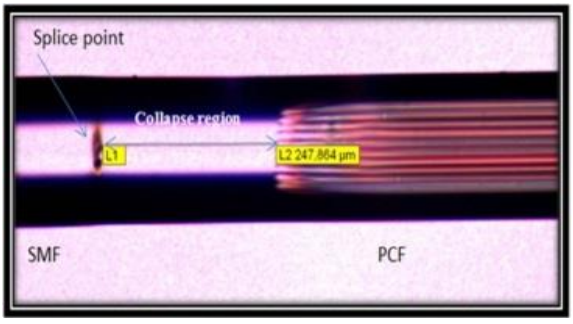


**Fig .1** Microscope image of the PCF collapsing interferometer

Humidity sensor based on transmission type of the PCFI was proposed. First, the coating of a stub of PCF (LM A-10 ) and conventional optical fiber (Corning, SMF-28) was removed by using a mechanical stripping. Then, the second step was cleaving the PCF and SMF, which was done by fiber cleaver. The third step was cleaning the fibers. Then, the stub of a (10 mm) long of commercial PCF was fusion spliced between two SMFs (Corning SMF-28) by a conventional splicing machine. After fusion splicing, the forth step was coating with agarose which was carried out by drawing the interferometer through a hot (65 $^{O}$C) agarose solution. The solution was prepared by dissolving 1 wt% agarose in distilled water. In order to undertake the coating process, the fiber was fixed straight and horizontally above a translation stage (TS). Below the fiber, a heater was fixed on a translation stage. A small container was placed at the top of the heater and was filled to the top with hot agarose solution as shown in Figure 2a and schematic a diagram of the experimental setup for agarose coating is shown in Figure 2b. The surface of the solution formed a dome-like shape which projects slightly above the rim of the container because of surface tension. The position of this container can be adjusted to allow the fiber to pass through this dome of agarose solution. The temperature of the heater was set at 65 $^{O}$C by temperature electrical controller system (TEC sys.). The fiber was drawn through the hot Agarose solution using a translation stage which was software controlled using a computer. This arrangement allowed good repeatability of the coating parameters.

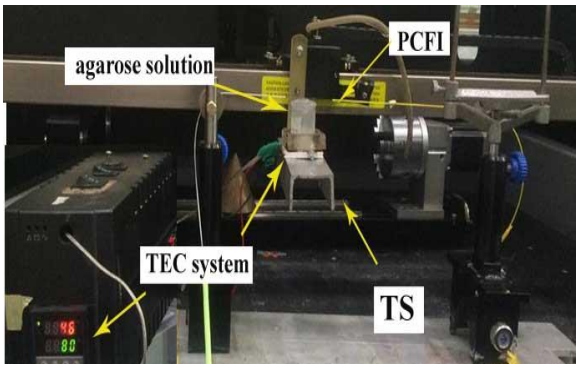


**Fig. 2.**a The photographic picture for setup of Agarose coating

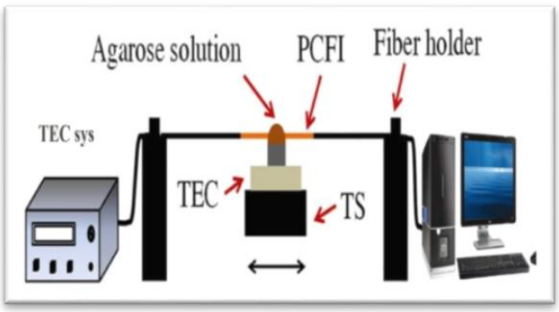


**Fig. 2.b** Schematic diagram of the experimental setup for Agarose coating

The light source (1550 nm) was launched into the interferometer through the SMF-PCF-SMF to the power meter or the Optical Spectrum Analyzer (OSA). The fabricated sensor responded to humidity variations was studied at room temperature and normal atmospheric pressure by putting it in an environmental chamber, which is a cuboid-shape sealed chamber, fabricated from Polyvinyl chloride (PVC) plastic. It consisted of dry/wet air flow system that can vary the internal humidity in the chamber (27%RH - 95% RH). There were three fans: the first fan pumped a dry air form a container containing a silica gel, the second fan pumped a wet air from container containing distilled water and heater (70 watt), and the last fan was on the surface of chamber to expel the air. A calibrated electronic humidity (XT9007-8 temperature & humidity control instrument) was used for monitoring the humidity and temperature inside the chamber as shown in Figures 3a and 3b.

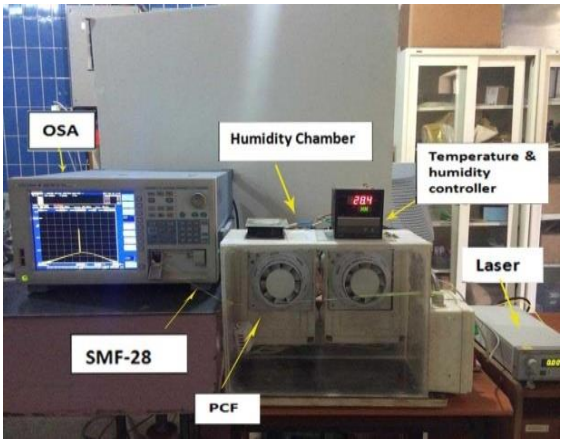


**Fig. 3.a** The photographic picture for the PCFI humidity sensor set up ( transmission type)

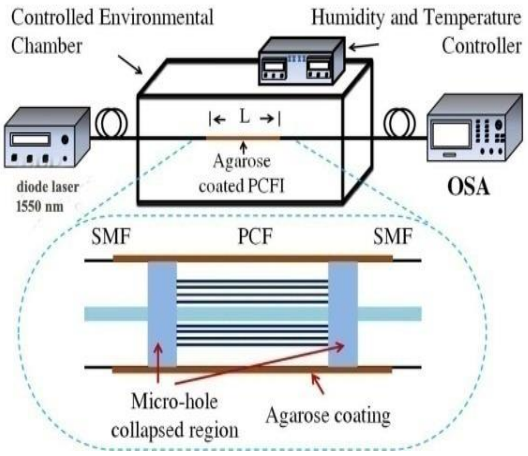


**Fig. 3.b.** Schematic of the humidity sensor system

## Results and Discussion

It was found that an uncoated PCFI that observed PCF with length (1cm) showed a higher sensitivity (0.239 pm/RH% ). The sensitivity was calculated from the linear fitting versus wavelength curve to RH (27%-85%). It was demonstrated that there was no wavelength shift based in Figures 4 and 5, in addition no decrease in transmitted power when increasing the RH <90 % as shown in Figure 6. This was because water has a hydrogen-bonded network (ice-like), which grows up as the relative humidity increases from 0% to 30 %. The liquid water structure starts appearing in the RH range of 30-60 %, while the structure of ice-like continues growing to saturation [27].

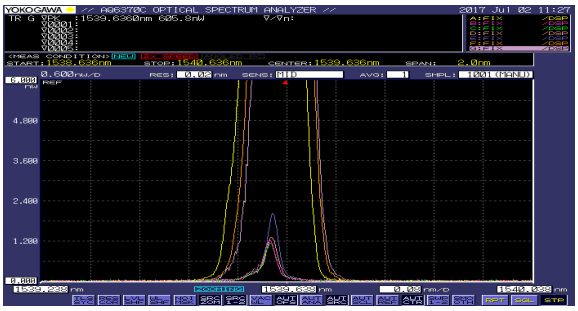


**Fig.4.** The shift in Wavelength peak of PCFI without coating in humidity chamber

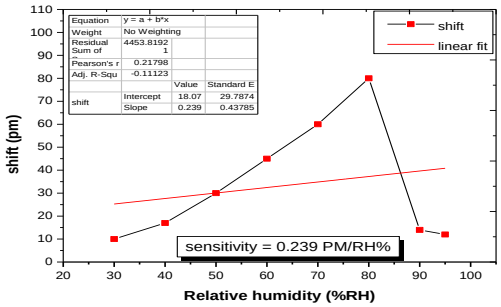


**Fig. 5.** Change in the transmission spectrum of a PCFI without coating of length 10mm with respect to different ambient relative humidity values.

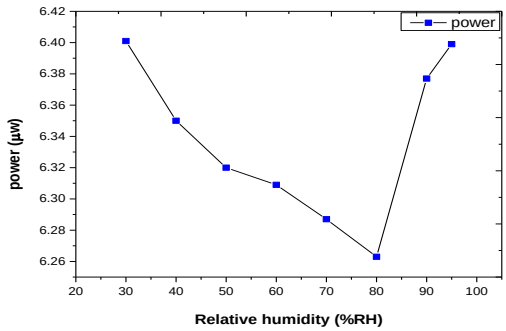


**Fig. 6.** Change in the transmission power of a PCFI without coating of length 10mm with respect to different ambient relative humidity values.

The agarose was coated in order to improve the humidity sensitivity of PCFI. The desired coating thickness can be achieved using this setup by varying the drawing speed of the fiber through the solution or by changing the viscosity (wt% of the agarose) of the solution or passing the fiber multiple times through the solution. The latter technique was found to be the best in order to achieve a suitable thickness and thus in this experiment, the fiber was drawn through the solution with a constant speed of 5 mm/sec . In practice after passing the fiber through the solution, the spectral red shift was observed in the transmission spectrum of the device compared with its initial spectrum as shown in Figures 7 and 8.

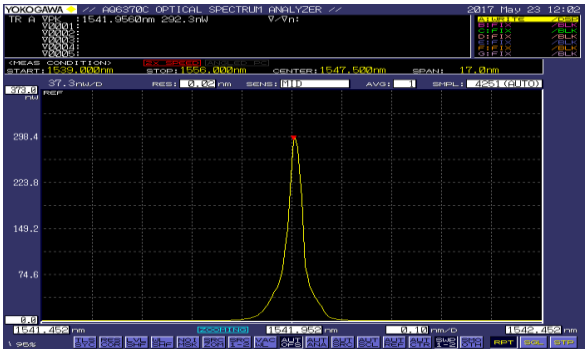

**Fig.7.** Wavelength peak of PCFI before coating

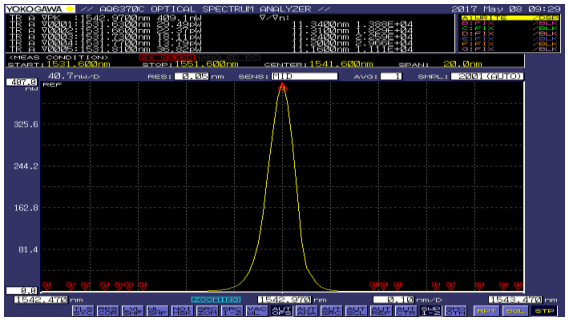

**Fig.8.** The shift in Wavelength peak of PCFI after coating is about 1.014 nm

.

The RH responses of the agarose Coating-PCFI devices were studied by placing them inside a controlled environmental chamber. The ambient temperature during the study was 25°C at normal atmospheric pressure. In these devices, the interaction of the coating was solely with the cladding modes since the core mode was isolated from the external environment. The interaction of the cladding modes with the agarose coating changed the effective index of the cladding mode and consequently the phase difference between the cladding mode and the core mode. As a result, the interference pattern shifted; that was the position of the interference peaks and valleys changed. An increase in the effective RI of the cladding mode causes a spectral red shift and a decrease in the effective RI causes a blue shift. The thickness change of the agarose coating for a change of RH the RI change as the thickness of the agarose coating and also increases when RH increases. When the RH level increases, more water molecules are diffused into the agarose coating, resulting in the inflation of the agarose and increased in the thickness of the coating. Similar to any other swelling polymer, an increase in water content will decrease the bulk refractive index of the agarose coating [28 ,29].To study the influence of the agarose film thickness on the properties of the PCFI, the four PCFI devices (A, B, C, D) previously fabricated were coated with different thicknesses of agarose film by passing the fiber through the solution multiple times. The thickness of the coated device was estimated using an optical microscope at a room RH of 40±2%. Table 1 shows parameters of the different AC-PCFI Devices

**Table 1.** Parameters of the Different AC-PCFI Devices

| AC-PCFI | A | B | C | D |
|---|---|---|---|---|
| Red peak shift ofthe coated PCFI relative tothe uncoated PCFI (nm) | 0.284 | 1.014 | 1.186 | 1.238 |
| No. of passes | 1 | 2 | 3 | 4 |
| The thickness of coating (nm ) | 300 | 630 | 3530 | 5966 |

When the coating thickness increased, the effective RI of the coating experienced by the cladding mode of the PCFI increased .As a result of the increase in the effect of the bulk, RI changed, resulting in a net red shift of the interference spectrum for all RH values and this was the case with the devices A and B in this experiment. Figure 9(a) shows the peaks shift of the interference pattern of the AC-PCFI A and B with respect to RH. The AC-PCFI A showed a spectral red shift with an increase in RH and the observed shift was linear in the range from 27 to 95% RH with a slope of 5.25914 pm/%RH. Above 90% RH, the sensitivity of the device is much higher most likely due to the water vapor condensation on the coating at these higher RH values. The AC-PCFI B showed a red shift with a slope of 7.937 pm/%RH in the range 27 to 95% RH. It can be concluded that when the thickness of the coating increases, the humidity sensitivity of the AC-PCFI also increases. In this experiment, it was observed that when the coating thickness is greater than ~750 nm, which was the case with AC-PCFI devices C and D, the observed shift was blue for the interference spectrum of the AC-PCFI device when the RH increased. For verification, the evanescent wave penetration depth of device C at 40% RH using Eq. (1)of reference [30] was calculated by setting the value of the RI of the fiber material silica, n1 = 1.44, the RI of the agarose coating n2 = 1.2213908 and assuming the angle of incidence at the fiber–coating interface $\theta$= 90°. Using these values the calculated penetration depth was756.09756 nm, verifying the observation that the wavelength shift changed from a red to a blue shift when the coating thickness was in the region of 750 nm.

$$\mathbf{dp} = \frac{\boldsymbol{\lambda}}{\mathbf{2\pi n_1}\left[\mathbf{\sin^2\theta - \frac{n_2^2}{n_1^2}}\right]^{1/2}} \ldots\ldots\ldots (\mathbf{1})$$

The humidity responses of the AC-PCFI devices C and D are shown in Figure 9(b). The ACPCFIC showed no spectral shift when humidity increases from 27% RH to 40% RH and then it showed a blue shift on a further increase of RH from 40% to 95% as seen from Figure 9(a). This was because below 40% RH, the thickness changed factor dominated by comparison to the bulk RI change of the coating and above 40% RH the coating thickness was greater than the penetration depth of the evanescent wave portion of the cladding mode interacting with the coating so that the effective RI of the cladding mode was mainly determined by the bulk RI of the coating. For AC-PCFI D, the peak wavelength phase changed point (RH at which the red shift changes to blue shift) of the RH response curve shifted to lower RH of 40% which was expected because here the coating was thicker than for AC-PCFI C that showed in Figure 9(b). For AC-PCFI D, the RI of the coating was in a more RI sensitive region of the PCFI and the RH sensitivity observed was also higher compared to other devices with a smaller thickness of agarose coating. The AC-PCFI D showed a sensitivity of -29.37394 pm/%RH in the range27-90%RH.

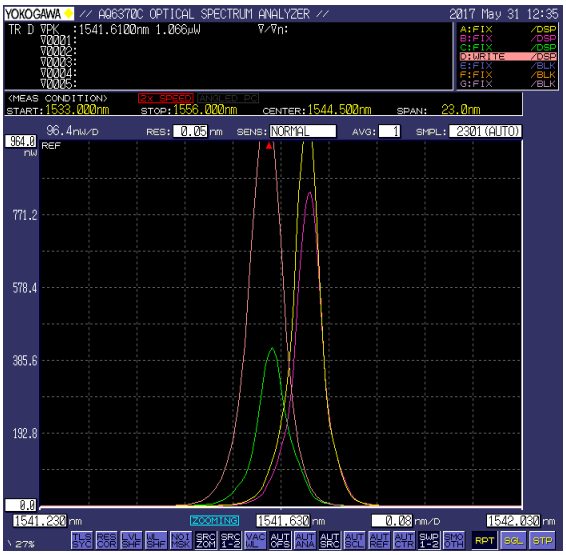


**Fig. 9. (a)** The shift in wavelength peak when the AC- PCFI C exposed to variable relative humidity

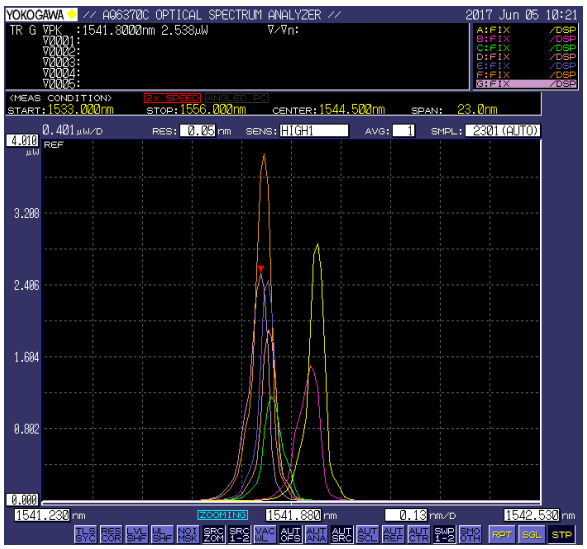


**Fig. 9. (b)** The shift in wavelength peak when the AC- PCFI D exposed to variable relative humidity

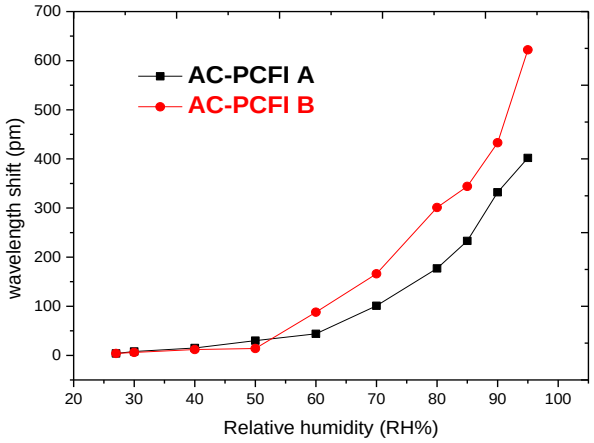


**Fig. 10. (a**) The spectral peak shift of AC-PCFI A and B with respect to relative

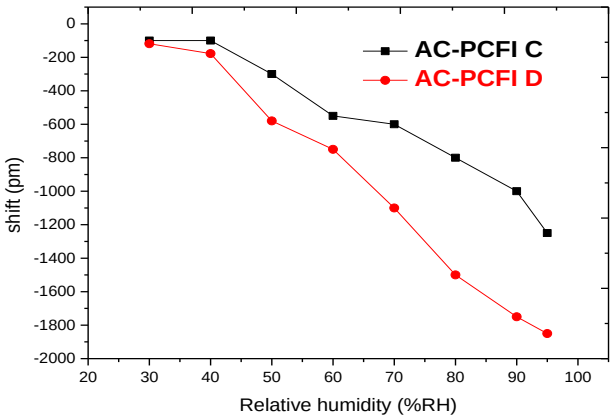


**Fig.10. (b**)The spectral peak shift of AC-PCFI C and D with respect to relative humidity.

The calculated RH sensitivities of the AC-PCFI devices in different linear RH regions are listed in Table 2, where the positive sensitivity values represent spectral red shift and negative values represent a blue shift.

**Table 2.** RH Sensitivity of AC-PCFI Devices

| **AC-PCFI** | **A** | **B** | **C** | **D** |
|---|---|---|---|---|
| Sensitivity (pm/%RH) | 5.25914 | 7.93756 | -17.3527 | -29.37394 |

To calculate the rise time of the sensor, AC-PCFI device D which shows a higher sensitivity to relative humidity variations was exposed to an environment with rapid changes of the RH. First, the RH in the chamber was kept at 50%, and then the humidity of the chamber was rapidly increased to 90 % (at room temperature and normal atmospheric pressure). The measured rise time of the sensor is shown in Figure 11. The sensor had a fast response to humidity variations and the estimated response time from 10 % to 90% of the signal maximum) was about 0.8 sec when the RH changed from 50% to 90 % at wavelength =1550nm.The recovery time of a humidity sensor depended on how fast the water vapor was removed from the sensor which was proportional to the air flow surrounding the sensor. The estimated recovery time (90% signal maximum to 10% baseline) of the sensor was 7 sec, which decreased if a flow of dry air surrounded the sensor.

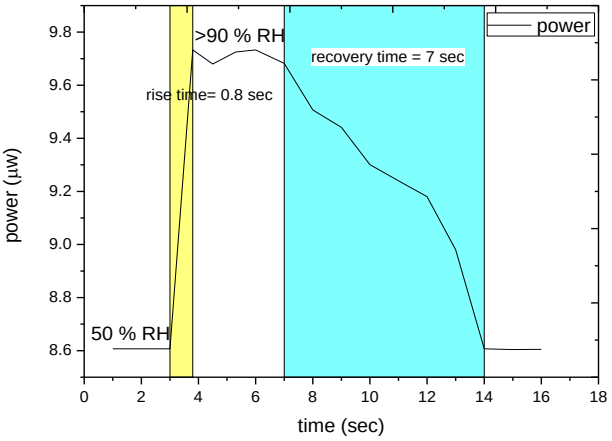


**Fig. 11.** Response time of the sensor.

## Conclusion

The AC-PCFI (transmission type) sensor has been demonstrated experimentally. An PCFI was coated with agarose layers of different thickness and showed the RI of the coating experienced by the mode interacting with the coating depended on the thickness of the coating. The effect of coating thickness on the RH response of the AC-PCFI devices was studied and that the RH sensitivity of an AC-PCFI depended strongly on the thickness of the coating. The sensor showed the highest sensitivity (-29.37394pm/%RH) at agarose coating thickness 5.966μm with a linear response for RH change in the range of 27-95%RH. The response time of the sensor was0.8 sec for an RH changed from 50% to 90%. This work also provided the basis for the selection of an optimal operating point in terms of sensitivity and a range of operation in the case of a PCFI coated with other materials for different sensing applications.

## References

[1] Tatara, T.; Tsuzaki, K. An apnea monitor using a rapid-response hygrometer. J. Clin. Monit. Comput., 13, 5–9,(1997).

[2] Lin, Y.C. "Breath sensor based on reflective optical lensed fiber". Microw. Opt. Technol. Lett., 55, 450–454,( 2013).

[3] Kastner, W.; Neugschwandtner, G.; Soucek, S.; Newmann, H.M. "Communication systems for building automation and control". Proc. IEEE , 93, 1178–1203,(2005).

[4] Laville, C.; Pellet, C. "Interdigitated humidity sensors for a portable clinical microsystem". IEEE Trans. Biomed. Eng., 49, 1162–1167,(2002).

[5] HabibAhsan, A.H.M.; Lange, C.F.; Moussa, W. "Development of a Humidity Microsensor with Thermal Reset". In Proceedings of the International Conference on MEMS, NANO and Smart Systems, Banff, AB, Canada, 20–23, pp. 89–93,July (2003).

[6] Tao Li, Xinyong Dong, Chi Chiu Chan, Chun-Liu Zhao, and PengZu"Humidity sensor based on a multimode-fiber taper coated with polyvinyl alcohol interacting with a fiber Bragg grating" IEEE Sensors J. 12, 2205–8(2012 ) .

[7] Mathew J, Semenova Y and Farrell G A fiber bend based humidity sensor with a wide linear range and fast measurement speed Sensors Actuators A 174 ,47–51,( 2012 ).

[8] Houhui Liang, Yongxing Jin, Jianfeng Wang,and Xinyong Dong Relative humidity sensor based on polarization maintaining fiber loop mirror with polymer coating Microw. Opt. Technol. Lett. 54 ,236, 4–6(2012).

[9] Li Han Chen, Chi Chiu Chan, Tao Li"Chitosan-coated polarization maintaining fiber-based Sagnac interferometer for relative humidity measurement" IEEE J. Sel. Top. Quantum Electron.18,1 ,597–604,(2012 ).

[10] Sandra F. H. Correia , Paulo Antunes , Edison Pecoraro , Patrícia P. Lima"Optical fiber relative humidity sensor based on a FBG with a di-ureasil coating Sensors"12 ,88, 47–60,(2012).

[11] Tong Sun, Kenneth T. V. Grattan, SudarshanSrinivasan, P. A. M. Basheer"Building stone condition monitoring using specially designed compensated optical fiber humidity sensors" IEEE Sensors J. 12, 101,1–7,( 2012).

[12] Li Xia Lecheng Li Wei Li Tian Kou Deming Liu"Novel optical fiber humidity sensor based ona no-core fiber structure Sensors" Actuators A ,190, 1–5,(2013).

[13]T. L. Yeo, T. Sun, and K. T. V. Grattan, "Fibre-optic sensor technologies for humidity and moisture measurement," Sens. Actuators A Phys. 144(2), 280–295,(2008).

[14] J. Mathew, K. J. Thomas, V. P. N. Nampoori, and P. Radhakrishnan, "A comparative study of fiber optic humidity sensors based on chitosan and agarose," Sens. Transducers J. 84, 1633–1640,(2007).

[15] H. Y. Choi, M. J. Kim, and B. H. Lee, "All-fiber Mach-Zehnder type interferometers formed in photonic crystalfiber," Opt. Express 15(9) 5711–5720,(2007),.

[16] M. Smietana, D. Brabant, W. J. Bock, P. Mikulic, and T. Eftimov, "Refractive-index sensing with inline core cladding intermodal interferometer based on silicon nitride nano-coated photonic crystal fiber," J. Light wave Technol. 30(8), 1185–1189, (2012).

[17] J. Villatoro, V. Finazzi, V. P. Minkovich, V. Pruneri, and G. Badenes, "Temperature-insensitive photonic crystal fiber interferometer for absolute strain sensing," Appl. Phys. Lett. 91(9), 091-109,(2007).

[18] R. Jha, J. Villatoro, and G. Badenes, "Ultrastable in reflection photonic crystal fiber modal interferometer for accurate refractive index sensing," Appl. Phys. Lett. 93(19), (2008),191-106 .

[19] J. Mathew, Y. Semenova, and G. Farrell, "Relative humidity sensor based on an agarose

infiltrated photonic crystal fiber interferometer," IEEE J. Sel. Top. Quantum Electron. 18(5) 1553–1559,(2012).
[20] D. Barrera, J. Villatoro, V. P. Finazzi, G. A. Cardenas-Sevilla, V. P. Minkovich, S. Sales, and V. Pruneri, "Low loss photonic crystal fiber interferometers for sensor networks," J. Light wave Technol. 28(24), 3542–3547,(2010).
[21] R. Jha, J. Villatoro, G. Badenes, and V. Pruneri, "Refractometry based on a photonic crystal fiberinterferometer," Opt. Lett. 34(5), 617–619,(2009).
[22] J. Mathew, Y. Semenova, and G. Farrell, "Polymer coated photonics crystal fiber interferometer for relative humidity sensing," A. Ghosh, and D. Choudhury (Eds.): Proc. IConTOP–II, 73–78,(2011).
[26] SALAHA. ADNAN , AHMED W. ABDULWAHHAB , SHAYMAA N. ISMAIL" Fusion splicing the penalty of increasing the collapse length of the air holes in ESM-12B photonic crystal fibers "Optica Applicata, XLVI, 2, 266-270, (2016 ) .
[27] B. David, H.Seong, J. Phys. Chem. B, 109, 35, 16, 760–16763, (2005).
[28] Mathew J, Semenova Y and Farrell G , OPTICS EXPRESS, 21,5, 6317,March( 2013).
[29] J. J. Roberts, A. Earns haw, V. L. Ferguson, and S. J. Bryant, "Comparative study of the viscoelastic mechanical behavior of agarose and poly(ethylene glycol) hydrogels," J. Biomed. Mater. Res. B Appl. Biomater. 99B(1),158–169,(2011).
[30] J. Lu, Z. Chen, F. Pang, and T. Wang, "Theoretical analysis of fiber-optic evanescent wave sensors," in Proceedings of IEEE Microwave Conference, (China-Japan Joint, 2008), doi: 10.1109/CJMW.4772500,583–587, (2008) .

## تحسين أداء الحساسية لمتحسس الرطوبة المستند على مقياس تداخل الليف الفوتوني البلوري ذو نمط النفاذية

**حسن فالح حسن  حنان جعفر طاهر**

معهد الليزر للدارسات العليا، جامعة بغداد، بغداد ، العراق

**الخلاصة:** مقياس التداخل للألياف البلورية الفوتونية تستعمل بشكل واسع في تطبيقات التحسس . وفي هذا العمل تم توصيف وتصنيع متحسس الرطوبة النسبية بالاعتماد على مقياس التداخل لماخ زيندر عند طلائه ببوليمر والذي يعمل في نمط النفاذية . تم تصنيع هذا المتحسس ببساطة بواسطة لحام ليف مقياس التداخل لليف الفوتوني البلوري ( LMA-10) ذو طول (1 سم ) بين ليفين ذات نمط مفرد ( SMF-28 ) .بعدها يتم طلاء الليف الفوتوني البوري بطبقة من محلول الاكاروس . من خلال النتائج التجريبية أبدى المتحسس حساسية عالية لمقدار التغير بالرطوبة (27%- 95% ) وقد حصل على اعلى مقدار للحساسية (29.37-) بيكو متر / النسبة المئوية للرطوبة النسبية. وقد اثبت ان متحسس الرطوبة المصمم يعتمد على سمك طبقة الطلاء و له عدة مزايا حجمه صغير , مستقر ، ذو قياسات دقيقية ، متحسس لمدى واسع من الرطوبة ،استجابة خطية لمقدار تغير الرطوبة , زمن الاستجابة سريع ( 0.8 ) ثانية للتغير من (50%- 90% ).